Photochemical & Photobiological Sciences
https://doi.org/10.1007/s43630-022-00309-w

ORIGINAL PAPERS

Visible light-driven degradation of Acid Orange 7 by light modulation techniques

Diana Sannino[1] · Nicola Morante[1] · Olga Sacco[2] · Antonietta Mancuso[1] · Luca De Guglielmo[3] · Giulia Di Capua[4] · Nicola Femia[3] · Vincenzo Vaiano[1]

Received: 15 July 2022 / Accepted: 19 September 2022

Abstract

The impact of light modulation on the decolorization of Acid Orange 7 (AO7) in aqueous solution was examined in this paper. A fixed bed batch photocatalytic reactor with a flat plate geometry, irradiated by 240 white-light LEDs, was used. A successful transfer of visible active photocatalyst (N-TiO_2) in powder form on a polystyrene (PS) transparent plate was realized. The structured photocatalyst was characterized through SEM–EDX, Raman and UV-DRS analyses, evidencing the formation of a coating of N-TiO_2 in the anatase phase, with a band-gap energy of 2.5 eV, and almost uniform distribution on the PS surface. Different LED dimming techniques, with fixed and variable duty-cycle values, were tested, and four types of light modulation were compared: fixed duty cycle (constant irradiation), sinusoidal variable duty cycle (sinusoidal variable irradiation), triangular variable duty cycle (triangular variable irradiation), and square wave variable duty cycle (square wave variable irradiation). The resulting responsiveness/efficiency of the LED versus the current intensity was evaluated, and the stability of the photocatalyst activity and the influence of optimized irradiation waveforms were examined in the decolorization of 400 mL of 10 ppm AO7 solution. The sinusoidal modulation, with current between 50 and 100 mA and 10 s as the period, shows the highest value of the apparent pseudo-first-order kinetic constant, resulting equal to 0.0044 min^{-1}, at parity of total transmitted photons. An energy saving with the application of sinusoidal irradiation is highlighted with respect to the literature.

✉ Diana Sannino
dsannino@unisa.it

✉ Giulia Di Capua
giulia.dicapua@unicas.it

[1] Department of Industrial Engineering, University of Salerno, Via Giovanni Paolo II 132, 84084 Fisciano, SA, Italy

[2] Department of Chemistry and Biology "A. Zambelli", University of Salerno, Via Giovanni Paolo II, 132, 84084 Fisciano, SA, Italy

[3] Department of Information, and Electrical Engineering and Applied Mathematics, University of Salerno, Via Giovanni Paolo II 132, 84084 Fisciano, SA, Italy

[4] Department of Electrical and Information Engineering "Maurizio Scarano", University of Cassino and Southern Lazio, Via G. Di Biasio 43, 03043 Cassino, FR, Italy

Published online: 01 October 2022

Graphical Abstract

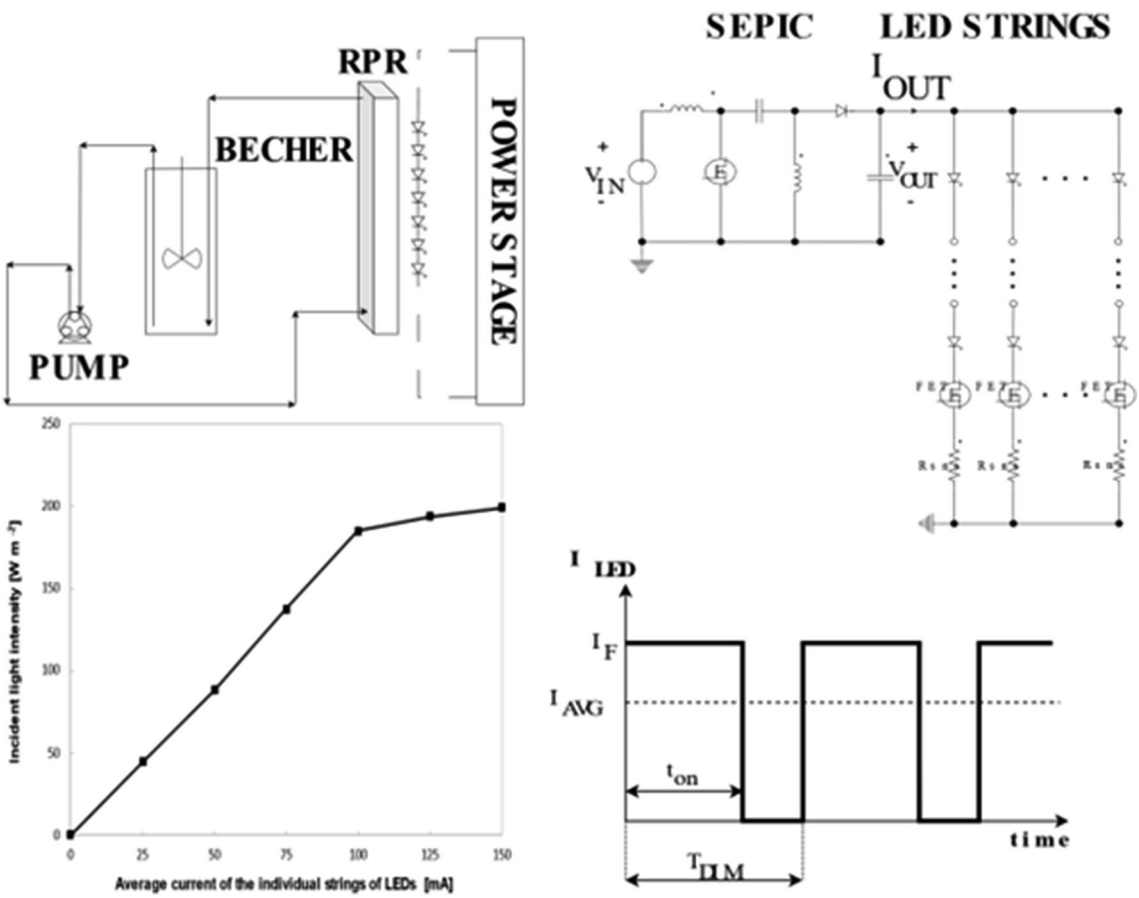

Keywords Light dimming techniques · Azo-dye photocatalysis · N-TiO_2 · Structured photocatalyst · Electrical energy per order

1 Introduction

The growth of pollution and the decrease of fresh water have raised the standards of the discharge of wastewater, so the individuation of technologies that allow the complete purification of hazardous wastewater has vital importance [1, 2]. Among the different pollutants, the azo dyes, due to their recalcitrant and inhibitory nature, cannot normally be degraded by conventional biological wastewater treatments [3].

Different types of organic dyes from the textile, paper and leather industries are discharged in liquid streams. One of the new and cost-effective methods for the removal of these contaminants from wastewater is Advanced Oxidation Processes (AOPs), quite effective for industrial and toxic wastewater treatments. Among the available AOPs, heterogeneous photocatalysis has proved to be a promising method for water purification [4, 5]. Indeed, the photocatalytic process, using a structured photocatalyst, is a sustainable purification method that respects the twelve principles of Green Chemistry proposed by Warner and Anastas [6]. Photocatalysis can be conducted under ambient conditions using titanium dioxide (TiO2) semiconductor as photocatalyst with sunlight and atmospheric oxygen [7]. TiO2 is non-toxic, highly active, cheap, sustainable and stable under a wide range of chemical conditions but it is limited by its wide band-gap (~3.2 eV), which requires ultraviolet light irradiation for activation [8]. Hence, it is necessary to extend the photo-response of TiO2 to the visible spectrum through modification of its structure, being one method of the doping of TiO2 lattice with non-metallic elements [9, 10].

The semiconductor nanopowders are usually used in slurry reactors with several disadvantages: the recirculation pumps have a limited utilization time due to corrosion and the final separation of photocatalyst from treated water is

achieved with high energy demand [11]. So, fixed bed photoreactors with structured photocatalysts are more favorable. The irradiation mode of the photocatalysts play also a significant role in the conversion rate of pollutants. Indeed, alternating light and dark periods give rise to improved photonic efficiency, reducing the recombination rate of the photogenerated pairs [12]. Therefore, the controlled periodic illumination represents an interesting approach to increase the photonic efficiency in photocatalytic processes and realizing the intensification of the process [13]. Light Emitting Diodes (LEDs) are the best sources to be modulated [14], and they can be electronically tuned by using LED dimming techniques, permitting light switch-on and switch-off on a microsecond time-scale.

In our previous works [15–18], it was observed that visible irradiation with the modulation of visible LEDs dimming duty cycle remarkably enhanced the photocatalytic performances towards methylene blue, urea and terephthalic acid degradation. To our best knowledge, the use of LED dimming duty-cycle modulation techniques in a photocatalytic system to photodegrade the azo dye Acid Orange 7 (AO7), using a visible light active structured photocatalysts in a flat plate photoreactor, has never been reported. For this reason, the aim of this work is to investigate the influence of controlled modulation of LED light dimming on the performances of a photocatalytic reactor for AO7 treatment using visible active photocatalyst (N-doped TiO2) immobilized on a polystyrene plate and to test the stability of photocatalyst.

2 Materials and methods

2.1 Preparation of the Structured Photocatalyst (N-TiO_2/PS)

The powder of N-doped TiO_2 (N-TiO_2) was prepared by direct hydrolysis of titanium tetraisopropoxide with ammonia aqueous solutions followed by calcination in air at 450 °C for 25 min [19]. In the preparation of the photocatalyst, the N/Ti molar ratio equal to 12 was used. The physical and optical characterization of N-TiO_2 in powder form showed that the main crystalline form was anatase, and the band-gap energy was equal to 2.5 eV [20].

The support used for the dispersion of the photocatalytic powder was a polystyrene plate (31 × 11x0.2 cm in size). The structured photocatalyst, named N-TiO_2/PS, was prepared by a solvent-assisted procedure according to the methods reported in our previous work [21, 22]. Initially, 1.7 g of N-TiO_2 photocatalyst was dispersed in 40 mL of acetone and sonicated. Subsequently, the suspension was spread onto the surface of the support using a Gilson micropipette at room temperature. Thanks to action induced by acetone which act as a solvent for the polystyrene, N-TiO_2 particles adhered to the external surface of PS plate. Finally, N-TiO_2/PS plate was dried at room temperature for 24 h. The amount of photocatalyst coated on PS pellets was measured by an analytical balance (Ohaus Mettler Toledo, 0.1 mg resolution), and the final loading of N-TiO_2 was found to be about 3 wt%.

2.2 Experimental set-up for photocatalytic tests

To evaluate the influence of light modulation on the efficiency of the water treatment process, a batch system composed of a recirculating photocatalytic reactor (RPR) (30 × 20x5 cm) irradiated by a matrix of 240 white-light LEDs was used. The flat geometry of the photoreactor guarantees the efficient excitation of structured photocatalyst by minimizing the photons loss inside the core of the reactor and, therefore, optimizing the photonic flow inside the photocatalytic bed [15].

A matrix of white-light LEDs, fixed on the photoreactor pyrex window, allows the irradiation of the structured photocatalyst without the dispersion of light around. The 24 strings of 10 LEDs in series are fixed on a heatsink and connected to a digitally controlled LED driver. Every string of LEDs is powered independently, and the light modulation is implemented by the LED driver. The white LEDs used are CREE MLCAWT-H1-0000-000XE1. They irradiate a typical nominal luminous flux 55.2 lm with a typical forward voltage drop 3.5 V at 200 mA DC current and luminous irradiation peak spectral emission at 445 nm wavelength. A simplified scheme of the experimental apparatus is shown in Fig. 1.

400 mL of aqueous solution with an initial AO7 concentration of 10 ppm has been introduced in a stirred tank. A recirculation liquid flow rate of 28 mL min−1 has been realized by the peristaltic pump. The liquid stream flows over the surface of the structured photocatalyst and emerged from the top of the reactor, going then into the tank, equipped with a magnetic stirrer. The initial interval of dark condition (dark phase) lasted the first 60 min, during which the adsorption–desorption equilibrium of the azo dye on the photocatalyst surface was achieved. Then, the LEDs were turned on (light phase) and, in the following 180 min, aqueous samples were periodically withdrawn. The AO7 concentration was measured by means of a PerkinElmer UV–vis spectrophotometer at a wavelength of 485 nm. Furthermore, the degree of mineralization was determined by measuring the total organic carbon (TOC) content of treated solutions samples at different times evaluating the total CO_2 evolved at high temperature (680 °C) through catalytic combustion on Pt/Al_2O_3 catalyst [23]. A radiometer (StellarNet) was used to measure the incident light intensity (W m^{-2}) emitted by the LED matrix as the average current of the individual strings of LEDs changes. In Fig. 2a saturation effects have been

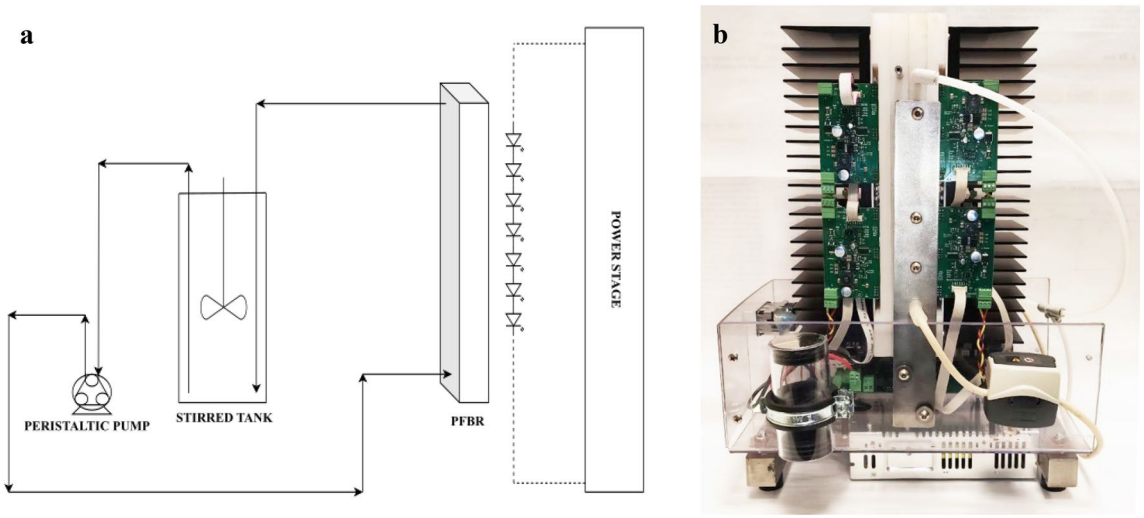

Fig. 1 **a** Experimental set-up scheme; **b** Picture of the photoreactor

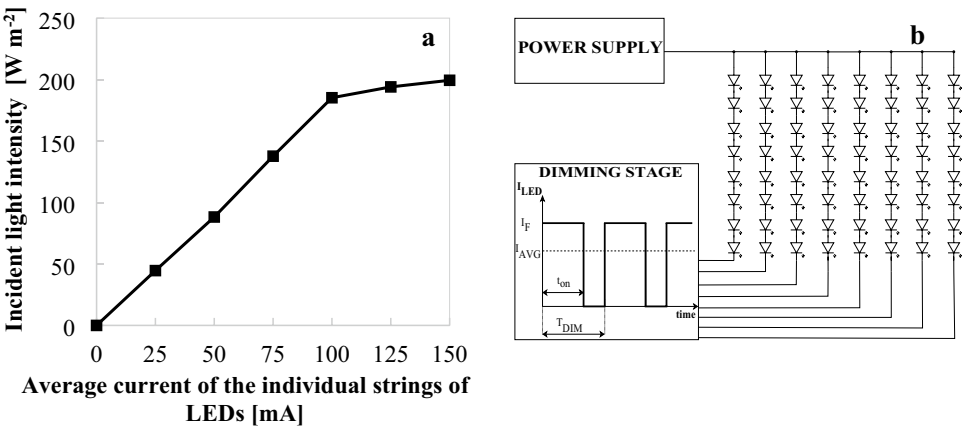

Fig. 2 **a** Incident light intensity as a function of the average supply current of the LED strings. **b** Scheme of dimming stage and LEDs strings

observed due to the decrease in the responsiveness/efficiency of the LED as the current intensity increases [24]. This highlights that it is not advantageous to supply the light source with a current greater than 100 mA.

2.3 Dimming techniques for light modulation

Light modulation is implemented by varying the duty cycle of the square wave dimmed the current intensity of the LED strings, by means of a dedicated LED driver module. This consists of a power unit, providing a regulated voltage V_{out}, and a dimming stage, which periodically turns on and off the current of each LED string with a dimming frequency f_{dim} = 20 kHz. This results in an average current regulation following the time variation of the duty cycle d_{dim}, defined as the ratio between the LED conduction time (t_{ON}) and the total duration of the dimming period (T_{dim}) [15]:

$$d_{dim} = \frac{t_{ON}}{T_{dim}}. \quad (1)$$

When LEDs are turned on, the peak current value of LED strings I_f at the value 200 mA. Therefore, the average current flowing (I_{avg}) in each single LED string is equal to:

$$I_{avg} = d_{dim} I_f, \quad (2)$$

where I_f is the on-state LED current and d_{dim} is the dimming duty cycle, as shown in Fig. 2 b.

Then, the light intensity was modulated over time by varying the value of d_{dim} at a fixed on-state LED current I_f. Specifically, four types of light modulation were used: fixed duty cycle (FD) (constant irradiation), sinusoidal variable duty cycle (S-VD) (sinusoidal variable irradiation), triangular variable duty cycle (T-VD) (triangular variable irradiation),

and square wave variable duty cycle (SW-VD) (square wave variable irradiation).

The following expressions describe the time dependence of the duty cycle for the various modulations tested:

$$d_{dim,\,S-VD}(t) = D_{DC} + D_{AC}\left(\sin\left(\frac{2\pi}{T_{dim}}t\right)\right), \tag{3}$$

$$d_{dim,\,T-VD}(t) = D_{DC} + D_{AC} \cdot \mathrm{abs}\left[\left(\left(t - \frac{T_{dim}}{4}\right)\mathrm{mod}\left(T_{dim}\right)\right) - \frac{T_{dim}}{2}\right] \tag{4}$$

$$d_{dim,\,SW-VD}(t) = D_{DC} + D_{AC} \cdot \mathrm{sgn}\left(\sin\left(\frac{2\pi}{T_{dim}}\right)t\right), \tag{5}$$

$$D_{DC} = (D_{max} + D_{min})/2, \tag{6}$$

$$D_{AC} = (D_{max} - D_{min})/2, \tag{7}$$

where D_{min} and D_{max} are minimum and maximum values for the dimming duty cycle, respectively. Since I_f is fixed, the average LED current, I_{avg}, and the incident light intensity, Φ, show the same law as the dimming duty cycle.

3 Results and discussion

3.1 Structured photocatalyst characterization

Figure 3 collects the morphological, optical and physical–chemical characterization of pristine polystyrene plate (PS TQ) and of structured photocatalyst N-TiO_2/PS. SEM image of PS plate is reported in Fig. 3a, showing a very smooth surface, free of any roughness. The surface of N-TiO_2/PS (Fig. 3b) is full of nanoparticle aggregates, demonstrating the anchoring of photocatalyst. The examined area of N-TiO_2/PS sample by EDX analysis is reported in Fig. 3c while the sum spectrum in Fig. 3d, where is possible to observe, apart from the signal of metal used for metallization (Cr and V), the presence essentially of Ti and O. They result well distributed on the surface as found in Fig. 3e and f, respectively. Raman spectra of pristine PS plate and N-TiO_2/PS structured photocatalyst are reported in Fig. 3g, where the main Raman bands of TiO_2 in anatase phase are evinced, superimposed to the bands of polystyrene. Only a residual weak band at around 1000 cm^{-1} is observable on the composite sample. Kubelka Munk spectra of pristine PS plate and N-TiO_2/PS photocatalyst reveal that composition of absorptions among the polystyrene, at around 280 nm, and the N-TiO_2 at 430 and 360 nm, is obtained. These results confirm the successful coating of PS surface with a N-TiO_2 nanoparticles film, whose characteristics were in agreement with those found in previous work [19, 25].

3.2 Preliminary analysis: stability

Initially, the performance of RPR for AO7 solution discoloration and the stability of N-TiO_2/PS were investigated using visible light irradiation at fixed duty (FD) LED dimming, where the fixed on-state LED current and the dimming duty cycle was fixed at 200 mA and 0.5, respectively, to get the values of incident light intensity equal to 200 ± 5 W m^{-2}.

Figure 4a underlines the stability of the photocatalyst. In fact, after 3 h of irradiation, the AO7 discoloration efficiency was unchanged with a value of about 55%, in the various cycles of activity tests. The level of mineralization during the stability tests is expressed in terms of TOC removal and is compared to the color removal in Fig. 4c. It is possible to observe that the final values of TOC removal efficiency resemble those of the color removal showing little differences. So total conversion to CO_2 and water is for the most obtained, with a little presence of intermediates.

3.3 Influence of the incident light intensity

Subsequently, the photodegradation of azo dye was analyzed using visible light irradiation at fixed duty LED dimming (FD). The average current flowing in each individual LED string (I_{AVG}) was fixed in the range 25–150 mA to obtain different values of incident light intensity (45 ± 5–199 ± 5 W m^{-2}) (Fig. 2a). The experimental data follow pseudo-first-order kinetics, as also confirmed by the literature about AO7 degradation [26].

Through a mass balance on the batch reaction system and integration, it was evaluated the apparent decolorization kinetic constant (k_{dec}) by the slope of the straight line obtained from plotting $F(t)$ vs time t (Eq. 8).:

$$k_{dec}(\Phi) = -\frac{\ln\left(\frac{c(t)}{c(t_0)}\right)}{t} = \frac{F(t)}{t}, \tag{8}$$

where k_{dec} is the apparent decolorization kinetic constant (min^{-1}) and $c(t)$ is the concentration of AO7 at any given time (ppm), t_0 is the initial irradiation time.

The value of the apparent kinetic constant is fixed at a constant temperature but depends on the intensity of irradiation (Φ), so it is expected to vary. The k_{dec} values (Fig. 4b) highlighted that with the increase of I_{AVG} from 25 to 100 mA, the apparent decolorization kinetic constant gradually increases until reaching a maximum value ($k_{dec} = 0.0046$ min^{-1}), while the further increase of I_{AVG} (100–150 mA) does not promote the kinetics [24], as

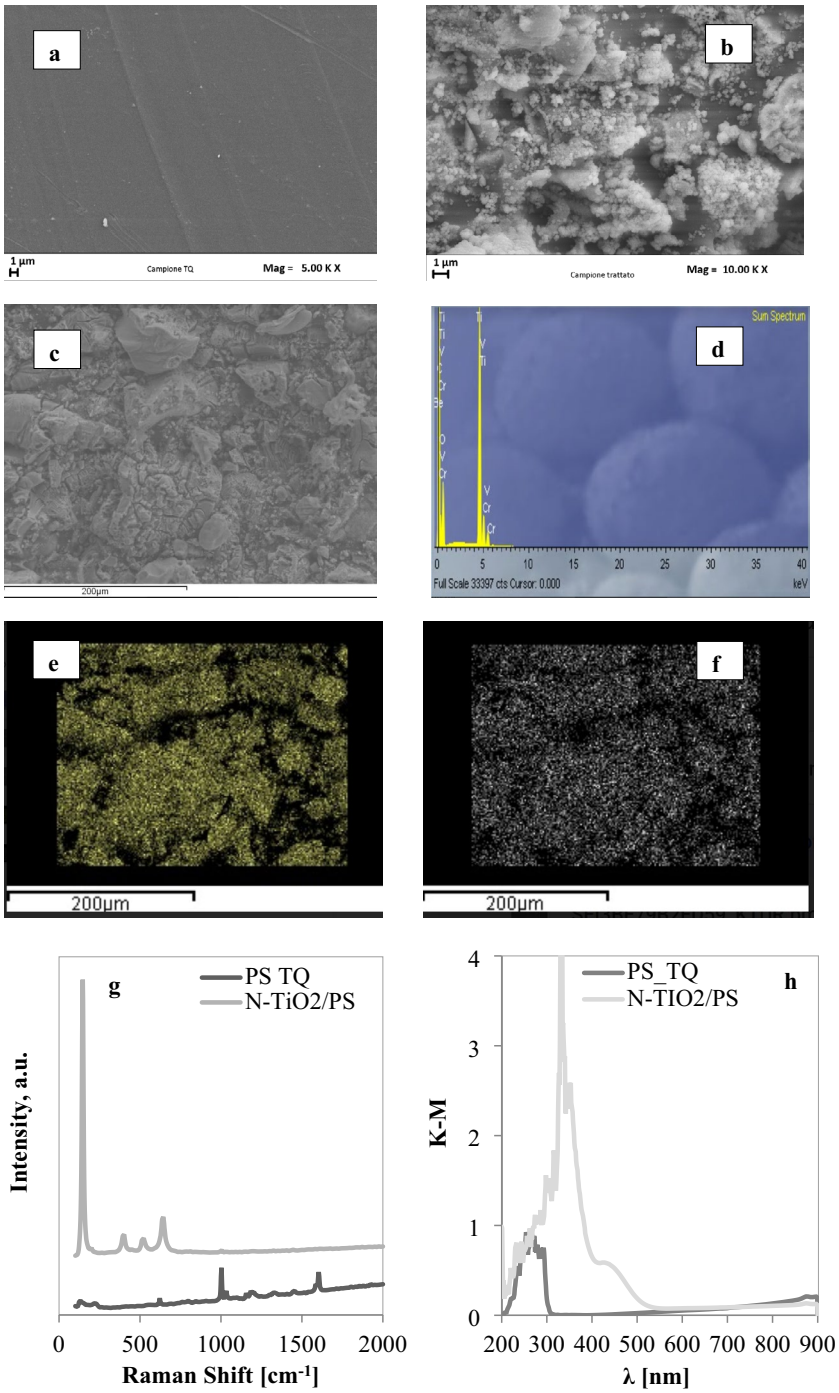

Fig. 3 **a** SEM image of PS plate. **b** and **c** SEM images of N-TiO_2/PS at different magnification. **d** EDX analysis at **c** magnification. **e** Ti mapping by EDX.f) O mapping by EDX. **g** Raman spectra of pristine PS plate (PS TQ) and N-TiO_2/PS structured photocatalyst. **h** Kubelka–Munk of pristine PS plate (PS TQ) and N-TiO_2/PS structured photocatalyst

expected due to the saturation effects caused by the decrease in the responsiveness/efficiency of the LEDs, as the current intensity increases further. For this reason, the tests of photocatalytic activity with the different dimming modulations were conducted with the maximum average current flowing in each LED string equal to 100 mA.

3.4 Influence of the period (*T*) on sinusoidal irradiation

The period of light modulations (*T*) is defined as equal to the time interval between two maximum peaks of the average current fed to the light source and, therefore, of the incident light intensity. The influence of the period of the modulated light, which varied in a sinusoidal way in the range of 50–100 mA. was examined, and the values of the

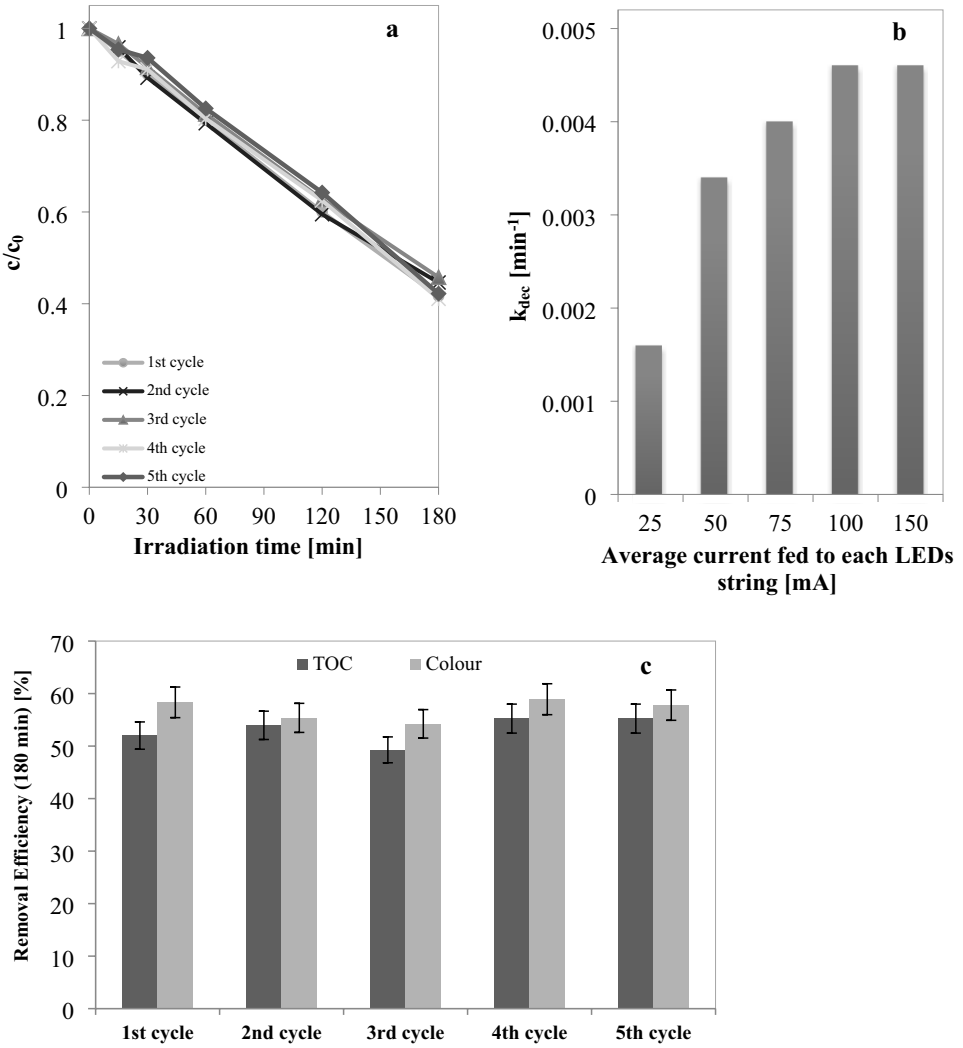

Fig. 4 **a** Stability of structured photocatalyst in the decolorization of AO7 under FD LED dimming. **b** Trend of the apparent kinetic constant as a function of the average current fed to each LEDs string. **c** Comparison of TOC and color removal efficiency at 180 min across the different stability tests

apparent kinetic constant were, respectively 0.0041, 0.0042, and 0.0044 min^{-1} for T equal 0.25, 5, and 10 s.

3.5 Influence of the different light modulations

Subsequent tests were conducted to evaluate the influence of the different light modulations on the photocatalytic activity. The modulations examined were triangular variable duty cycle (T-VD), and square wave variable duty cycle (SW-VD) both with an average current between 50 and 100 mA and a period of light modulation equal to 10 s (See Fig.S1 in Supplementary Material). The corresponding k_{dec} values were 0.0035–0.0036 min^{-1}, lower than that obtained with the optimized sinusoidal modulation (0.0044 min^{-1}), highlighting that the best activity is achieved using sinusoidal modulation.

3.6 Electric energy consumption evaluation

Finally, the electric energy consumption related to the photodegradation of 90% of AO7 in 1 m^3 of contaminated water was evaluated for the tests conducted by feeding an average current of 75 mA to each LEDs string. This analysis was performed using the correlation of Bolton et al. [27]:

$$E_{E/O} = \frac{P\ t\ 1000}{V\ 60 \ln\left(\frac{c(t_0)}{c(t)}\right)}, \quad (9)$$

where P is the nominal power of the light source (kW), t is the irradiation time to obtain a 90% removal of AO7 (min), V is the solution volume treated (L), $c(t_0)$ is the AO7 concentration at the initial irradiation time (ppm) and $c(t)$ is the AO7 concentration at the irradiation time t (ppm).

The calculated values of electric energy consumption for the different light modulations are shown in Table 1, compared at the fixed global amount of photons sent on the photocatalyst during the different tests. From this analysis,

Table 1 Electric energy consumption for the reduction of 90% of the AO7 in 1m^3 of solution for the different light modulations by powering the LEDs strings with an average current of 75 mA

Light modulation	$I_{avg,\ min}$ [mA]	$I_{avg,\ max}$ [mA]	T [s]	TOC removal$_{180\ min}$ [%]	$E_{E/O}$ [kWh m^{-3}]
Fixed	75	75	-	43	625
Sinusoidal	50	100	10	44	568
Triangular	50	100	10	44	694
Square Wave	50	100	10	35	714

Table 2 Comparison of the energy cost for the reduction of 90% of the AO7 in 1 m^3 of solution for RPR illuminated with sinusoidal light modulation and other works

Photocatalytic system	Photo catalyst	P [kW]	k_{dec} [min^{-1}]	C_0 [ppm]	V [L]	$E_{E/O}$ [kWh m^{-3}]
Our system with sinusoidal light modulation	N-TiO_2	0.06	0.0044	10	0.4	568
[28]	P25	0.4	0.0006	100	0.07	158,203
[29]	P25	0.175	0.0086	40	0.45	758
[30]	P25	1	0.0050	35	0.2	16,667
[31]	$Bi_{12}TiO_{20}$	1	0.0059	20	0.08	35,311

it emerges that sinusoidal modulation is the most efficient in energy saving. The reason for this behavior could be related to the kinetics of the elementary steps of photodegradation of AO7, since a similar result has been ascribed to the limitation of the recombination of the photoexcited charge carriers, as evinced by mathematical modeling of the photoreaction [18]. It is worthwhile to note that the different light modulations permit similar TOC removal percentages after 180 min of irradiation (Table 1), except for the square wave modulation that presents a lower mineralization value.

In the literature, different works have been identified that use photocatalysis for the degradation of AO7 in aqueous solutions.

From Eq. 9, the $E_{E/O}$ value for the four systems was determined and compared in the case of optimal modulation of the light (sinusoidal modulation). The results are reported in Table 2.

Our photocatalytic system presents the greatest energetic efficiency. Indeed, it shows the greatest energy efficiency in the AO7 removal, using a fixed bed reactor and a visible light source, permitting a consistent energy saving.

4 Conclusions

A structured visible active photocatalyst was obtained on PS plate and implemented in a RPR specifically designed photoreactor. The characterization showed the presence of a coating on PS plate of a visible active photocatalyst which retains the characteristics of the powder. The stability of the photocatalyst was assessed after various cycles of tests under fixed irradiation where the photocatalytic activity has not been altered, showing the AO7 discoloration efficiency of about 57% after 3 h of fixed irradiation.

The obtained AO7 photodegradation results confirm that photocatalysis with modulated visible light is an extremely sustainable purification process with high efficiency in the photodegradation of pollutants. Light modulations of four types, fixed, triangular wave, square wave, and sinusoidal wave, were optimized and compared, the latter the most efficient in the photocatalytic decolorization of AO7.

The best modulation had a period of 10 s and average current intensity between 50 and 100 mA, showing an apparent kinetic constant of 0.0044 min^{-1}. Furthermore, photocatalytic tests demonstrated the improvement of the process energy efficiency using the optimized sinusoidal modulation of visible LED light sources, leading to a favorable energy cost per m^3 required for the abatement of 90% of the AO7. The evaluation of the energy costs of the depollution in comparison with the literature showed that the optimized irradiation permits a relevant saving due to better utilization of transmitted photons for the AO7 oxidation reaction, so limiting the charge carriers recombination phenomena.

Supplementary Information The online version contains supplementary material available at https://doi.org/10.1007/s43630-022-00309-w.

Acknowledgements The authors thank the spin-off company IPERA SRL, for the realization of the photoreactor.

Funding Open access funding provided by Università degli Studi di Salerno within the CRUI-CARE Agreement.

References

1. Wang, Z.-P., Xu, J., Cai, W.-M., Zhou, B.-X., He, Z.-G., Cai, C.-G., & Hong, X.-T. (2005). Visible light induced photodegradation of organic pollutants on nitrogen and fluorine co-doped TiO_2 photocatalyst. *Journal of Environmental Sciences, 17*, 76–80.
2. Daughton, C. G. (2001). Emerging pollutants, and communicating the science of environmental chemistry and mass spectrometry: Pharmaceuticals in the environment. *Journal of the American Society for Mass Spectrometry, 12*, 1067–1076.
3. Pagga, U., & Brown, D. (1986). The degradation of dyestuffs: Part II Behaviour of dyestuffs in aerobic biodegradation tests. *Chemosphere, 15*, 479–491.
4. Herrmann, J.-M. (1999). Heterogeneous photocatalysis: Fundamentals and applications to the removal of various types of aqueous pollutants. *Catalysis Today, 53*, 115–129.
5. Sannino, D., Rizzo, L., & Vaiano, V. (2017) Progress in nanomaterials applications for water purification. In *Nanotechnologies for Environmental Remediation*. pp. 1–24. Springer.
6. Anastas, P. T., & Warner, J. C. (1998) Principles of green chemistry. Green chemistry: Theory and practice. *Oxford University Press*, pp. 30.
7. Hoffmann, M. R., Martin, S. T., Choi, W., & Bahnemann, D. W. (1995). Environmental applications of semiconductor photocatalysis. *Chemical Reviews, 95*, 69–96.
8. Nakata, K., & Fujishima, A. (2012). TiO2 photocatalysis: design and applications. *Journal of Photochemistry and Photobiology C: Photochemistry Reviews, 13*, 169–189.
9. Cheng, H.-H., Chen, S.-S., Yang, S.-Y., Liu, H.-M., & Lin, K.-S. (2018). Sol-Gel hydrothermal synthesis and visible light photocatalytic degradation performance of Fe/N codoped TiO2 catalysts. *Materials, 11*, 939.
10. Mohseni-Salehi, M. S., Taheri-Nassaj, E., & Hosseini-Zori, M. (2018). Effect of dopant (Co, Ni) concentration and hydroxyapatite compositing on photocatalytic activity of titania towards dye degradation. *Journal of Photochemistry and Photobiology A: Chemistry, 356*, 57–70.
11. Vaiano, V., Sarno, G., Sacco, O., & Sannino, D. (2017). Degradation of terephthalic acid in a photocatalytic system able to work also at high pressure. *Chemical Engineering Journal, 312*, 10–19.
12. Sczechowski, J. G., Koval, C. A., & Noble, R. D. (1993). Evidence of critical illumination and dark recovery times for increasing the photoefficiency of aqueous heterogeneous photocatalysis. *Journal of Photochemistry and Photobiology A: Chemistry, 74*, 273–278.
13. Rasoulifard, M., Fazli, M., & Eskandarian, M. (2014). Kinetic study for photocatalytic degradation of Direct Red 23 in UV–LED/nano-TiO2/S2O82− process: dependence of degradation kinetic on operational parameters. *Journal of Industrial and Engineering Chemistry, 20*, 3695–3702.
14. Gayral, B. (2017). LEDs for lighting: Basic physics and prospects for energy savings. *Comptes Rendus Physique, 18*, 453–461.
15. Di Capua, G., Femia, N., Migliaro, M., Sacco, O., Sannino, D., Stoyka, K., & Vaiano, V. (2017). Intensification of a flat-plate photocatalytic reactor performances by innovative visible light modulation techniques: A proof of concept. *Chemical Engineering and Processing: Process Intensification, 118*, 117–123.
16. Vaiano, V., Sacco, O., Sannino, D., Di Capua, G., & Femia, N. (2017). Enhanced performances of a photocatalytic reactor for wastewater treatment using controlled modulation of LEDs light. *Chemical Engineering Transactions, 57*, 553–558.
17. Vaiano, V., Sacco, O., Di Capua, G., Femia, N., & Sannino, D. (2019). Use of visible light modulation techniques in urea photocatalytic degradation. *Water, 11*, 1642.
18. Sannino, D., Sacco, O., V Vaiano, V., Morante, N., De Guglielmo, L., Di Capua, G., & Femia, N. (2021) Visible light driven degradation of terephthalic acid: optimization of energy demand by light modulation techniques. *Journal of Photocatalysis,* pp. 49–61.
19. Sacco, O., Stoller, M., Vaiano, V., Ciambelli, P., Chianese, A., Sannino D. (2012) Photocatalytic degradation of organic dyes under visible light on N-doped TiO 2 photocatalysts. *International Journal of Photoenergy*, pp. 626759.
20. Sacco, O., Vaiano, V., Han, C., Sannino, D., & Dionysiou, D. D. (2015). Photocatalytic removal of atrazine using N-doped TiO2 supported on phosphors. *Applied Catalysis B: Environmental, 164*, 462–474.
21. Sacco, O., Vaiano, V., Rizzo, L., & Sannino, D. (2018). Photocatalytic activity of a visible light active structured photocatalyst developed for municipal wastewater treatment. *Journal of Cleaner Production, 175*, 38–49.
22. Vaiano, V., Matarangolo, M., & Sacco, O. (2018). UV-LEDs floating-bed photoreactor for the removal of caffeine and paracetamol using ZnO supported on polystyrene pellets. *Chemical Engineering Journal, 350*, 703–713.
23. Bahadori, E., Vaiano, V., Esposito, S., Armandi, M., Sannino, D., & Bonelli, B. (2018). Photo-activated degradation of tartrazine by H2O2 as catalyzed by both bare and Fe-doped methyl-imogolite nanotubes. *Catalysis Today, 304*, 199–207.
24. Bhattacharya, P. (1997) *Semiconductor optoelectronic devices.* Prentice-Hall, Inc. p.57.
25. Ata, R., Sacco, O., Vaiano, V., Rizzo, L., Tore, G. Y., & Sannino, D. (2017). Visible light active N-doped TiO2 immobilized on polystyrene as efficient system for wastewater treatment. *Journal of Photochemistry and Photobiology A: Chemistry, 348*, 255–262.
26. Mancuso, A., Sacco, O., Sannino, D., Pragliola, S., & Vaiano, V. (2020). Enhanced visible-light-driven photodegradation of Acid Orange 7 azo dye in aqueous solution using Fe-N co-doped TiO2. *Arabian Journal of Chemistry, 13*, 8347–8360.
27. Bolton, J. R., Bircher, K. G., Tumas, W., & Tolman, C. A. (2001). Figures-of-merit for the technical development and application of advanced oxidation technologies for both electric-and solar-driven systems (IUPAC Technical Report). *Pure and Applied Chemistry, 73*, 627–637.
28. Stylidi, M., Kondarides, D. I., & Verykios, X. E. (2004). Visible light-induced photocatalytic degradation of acid orange 7 in aqueous TiO2 suspensions. *Applied Catalysis B: Environmental, 47*, 189–201.
29. Wang, K., Zhang, J., Lou, L., Yang, S., & Chen, Y. (2004). UV or visible light induced photodegradation of AO7 on TiO2 particles: the influence of inorganic anions. *Journal of Photochemistry and Photobiology A: Chemistry, 165*, 201–207.
30. Chen, X., Wang, W., Xiao, H., Hong, C., Zhu, F., Yao, Y., & Xue, Z. (2012). Accelerated TiO2 photocatalytic degradation of Acid Orange 7 under visible light mediated by peroxymonosulfate. *Chemical Engineering Journal, 193*, 290–295.
31. Zhu, X., Zhang, J., & Chen, F. (2011). Study on visible light photocatalytic activity and mechanism of spherical Bi12TiO20 nanoparticles prepared by low-power hydrothermal method. *Applied Catalysis B: Environmental, 102*, 316–322.